HT-FED 2004
ASME/ FLUIDS ENGINEERING SUMMER CONFERENCE
Charlotte, North Carolina, USA. July 11-15 2004

56532

NUMERICAL SIMULATION OF MIXED CONVECTIVE FLOW OVER A THREE-DIMENSIONAL HORIZONTAL BACKWARD FACING STEP

J.G. Barbosa Saldana

Department of Mechanical Engineering
Texas A&M University
College Station, Texas 77843
Sponsor student at TAMU by ANUIES- IPN-MEXICO

N.K. Anand

Department of Mechanical Engineering
Texas A&M University
College Station, Texas 77843

V. Sarin

Department of Computer Science
Texas A&M University
College Station, Texas 77843

ABSTRACT

Laminar mixed convective flow over a three-dimensional horizontal backward-facing step heated from below at a constant temperature was numerically simulated using a finite volume technique and the most relevant hydrodynamic and thermal features for air flowing through the channel are presented in this work. The channel considered in this work has an aspect ratio AR=4, and an expansion ratio ER=2, while the total length in the streamwise direction is 52 times the step height (L=52s) and the step length is equal to 2 times the step height (*l*=2s). The flow at the duct entrance was considered to be hydro-dynamically fully developed and isothermal. The bottom wall of the channel was subjected to a constant high temperature while the other walls were treated to be adiabatic. The step was considered to be a thermal conductive block.

INTRODUCTION

Separation and reattachment flows is a phenomenon that is found in several industrial devices such as in pieces of electronic cooling equipment, cooling of nuclear reactors, cooling of turbines blades, flow in combustion chambers, flow in wide angle diffusers, and valves. In other situations the separation is induced in order to induce more favorable heat transfer conditions as in the case of compact heat exchangers [1-3].

In the last decade several numerical studies have been conducted to gain a better knowledge and understanding of the hydrodynamic and thermal aspect of the separated flow and the backward-facing step has been the main target of several researchers. Even though the geometry is simple it is rich in physics as it captures complex flow and heat transfer features associated with separation and reattachment. For this reason flow over a backward facing step has been used as a benchmark problem for validating numerical codes and numerical procedures [4].

Recent developments in terms of computing speed and memory storage have permitted the solution to problems that demand extremely high computational resources as in the case of numerical simulations of three-dimensional flows, including fluid flow and heat transfer phenomenon over a three-dimensional backward facing step problem [5-8]. However, none of the previously cited publications include the effects of buoyant forces or mixed convective flow, even though the

effects of buoyant forces become significant when dealing with laminar flow regime with strong temperature gradients.

The mixed convective flow over a three-dimensional backward facing step is not a very common topic found in the literature. Nie, Armaly, Li and collaborators [7, 9] have considered the effect of buoyancy force (mixed convection effects) in vertical ducts wherein the gravitational vector and flow direction are parallel.

Iwai et .al. studied mixed convection in vertical ducts with backward facing step by varying the duct angle of inclination [2]. However, their study was confined to extremely weak buoyancy forces. For example, when the backward facing step is aligned with the horizontal axis the modified Richardson number was chosen to be equal to 0.03 (Ri^*=0.03). This value is associated with buoyancy effects that are not strong enough to alter the velocity field and temperature distributions from the pure forced convection values. Therefore, the flow in the cited report can be judged and qualified as being a pure forced convective flow.

The work that comes close to the configuration considered in this study is that of Iwai et. al. [2]. Hence it is concluded that there is no work reported on mixed convective flows over a horizontal three-dimensional backward facing step to date in the literature.

In this work, numerical simulation of three-dimensional mixed convective air flow over a horizontal backward facing step heating from below at a constant temperature is presented. The simulation is carried out for dominant free convective flow and the results for limiting cases are compared with those of pure forced convective three-dimensional flow. Also, the back step is considered as a conductive block which is another unique aspect of this study.

Keywords

Numerical simulation, Backward-facing-step, Mixed convection

NOMENCLATURE

AR Aspect ratio, AR=W/s

Cp Specific heat

ER Expansion ratio, ER=H/(H-s)

g Acceleration due to gravity

Gr Grashof number, $Gr = \frac{g\beta\Delta T s^3}{\upsilon^2}$

H Channel height at the inlet

k Thermal conductivity

L Total length of the channel, L=52s

l Total length of the step, *l*=2s

Nu Average Nusselt number, $Nu = \frac{\left(d\bar{T}/dy\right)\Big|_{y=0} 2H}{(T_{wall} - T_b)}$

p Pressure

Pr Prandtl number

Re Reynolds number, $\mathrm{Re} = \frac{\rho U_0 2H}{\mu}$

Ri Richardson number, $Ri = \frac{g\beta\Delta T s^3}{\nu^2 \mathrm{Re}^2}$

Ri* Modified Richardson number, $Ri^* = \frac{g\beta q_0 s^4}{\nu^2 k \mathrm{Re}^2}$

s Step height

T Temperature

U_o Bulk velocity at the inlet

u Velocity component in x direction

v Velocity component in y direction

w Velocity component in z direction

W Channel wide

2H Channel height

$x_{u\text{-line}}$, $x_{u-line} = \left[\left(du/dy\right)_{z=const}\right]\Big|_{y=0}$

x, y, z Coordinate directions

Subscripts

b bulk

f Fluid

max Maximum

s Solid

0 Inlet

w Wall

Greek letters

α Underrelaxation factor

β Coefficient of thermal expansion

μ Dynamic viscosity

τ_{wx} Average streamwise shear stress, $\tau_{wx} = \mu\left(d\bar{u}/dy\right)\Big|_{y=o}$

υ Kinematic viscosity

ρ Density

MODEL DESCRIPTION AND NUMERICAL PROCEDURE

The geometry considered in this study is shown in Fig. 1. The duct aspect ratio and expansion ratio were fixed in relation to the step height (s) as AR=4 and ER=2 respectively. The total length of the channel is equal to 52 times the step height L=52s and the length of the step is fixed as two times the step height *l*=2s. This particular geometry was chosen to study the strong three-dimensional behavior of the flow over the backward facing step.

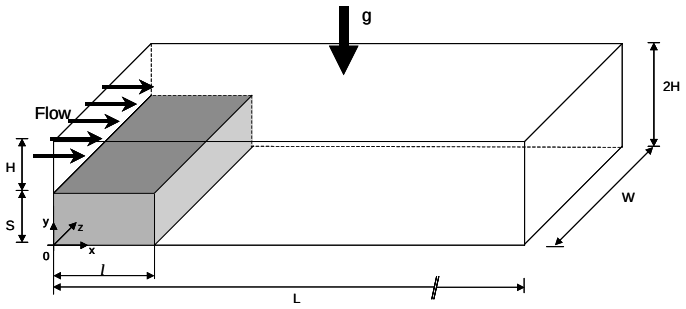

Fig. 1 Schematic of the 3-D backward facing step

Flow was assumed to be steady and the Boussinesq approximation was invoked to confine the variation for density in the flow. Based on these simplifying assumptions the steady three-dimensional mass conservation, momentum, and energy equations governing the fluid flow and heat transfer problem are reduced to the following forms: [10, 11]

Continuity Equation:

$$\frac{\partial(\rho u)}{\partial x}+\frac{\partial(\rho v)}{\partial y}+\frac{\partial(\rho w)}{\partial z}=0 \tag{1}$$

X Momentum Equation:

$$\left(u\frac{\partial(\rho u)}{\partial x}+v\frac{\partial(\rho u)}{\partial y}+w\frac{\partial(\rho u)}{\partial z}\right)= -\frac{\partial p}{\partial x}+\left(\frac{\partial}{\partial x}\left(\mu\frac{\partial u}{\partial x}\right)+\frac{\partial}{\partial y}\left(\mu\frac{\partial u}{\partial y}\right)+\frac{\partial}{\partial z}\left(\mu\frac{\partial u}{\partial z}\right)\right) \tag{2}$$

Y Momentum Equation:

$$\left(u\frac{\partial(\rho v)}{\partial x}+v\frac{\partial(\rho v)}{\partial y}+w\frac{\partial(\rho v)}{\partial z}\right)= -\frac{\partial p}{\partial y}+\rho_0\beta(T-T_0)g_y+\left(\frac{\partial}{\partial x}\left(\mu\frac{\partial v}{\partial x}\right)+\frac{\partial}{\partial y}\left(\mu\frac{\partial v}{\partial y}\right)+\frac{\partial}{\partial z}\left(\mu\frac{\partial v}{\partial z}\right)\right) \tag{3}$$

Z Momentum Equation:

$$\left(u\frac{\partial(\rho w)}{\partial x}+v\frac{\partial(\rho w)}{\partial y}+w\frac{\partial(\rho w)}{\partial z}\right)= -\frac{\partial p}{\partial x}+\left(\frac{\partial}{\partial x}\left(\mu\frac{\partial w}{\partial x}\right)+\frac{\partial}{\partial y}\left(\mu\frac{\partial w}{\partial y}\right)+\frac{\partial}{\partial z}\left(\mu\frac{\partial w}{\partial z}\right)\right) \tag{4}$$

Energy Equation:

$$\left(u\frac{\partial(\rho CpT)}{\partial x}+v\frac{\partial(\rho CpT)}{\partial y}+w\frac{\partial(\rho CpT)}{\partial z}\right)= \left(\frac{\partial}{\partial x}\left(k\frac{\partial T}{\partial x}\right)+\frac{\partial}{\partial y}\left(k\frac{\partial T}{\partial y}\right)+\frac{\partial}{\partial z}\left(k\frac{\partial T}{\partial z}\right)\right) \tag{5}$$

The Y momentum eq. (2) contains the buoyancy effects and according to the Boussinesq approximation the density variation due to the buoyancy effect is related to the volumetric thermal expansion coefficient (β) of the fluid.

At the duct entrance the flow was treated as fully developed [12] and isothermal. No-slip condition was applied at the duct walls, including the step walls. The bottom wall of the channel ($0\le x\le L$; $0\le z\le W$) was subjected to a constant temperature (T_w) and the rest of the walls were treated as adiabatic.

In this work the step was considered to be conducting with a thermal conductivity k_s. The conjugate problem of conduction-convection at the solid-fluid interface of the step was solved by a pseudo-solid-specific heat method as suggested by Xi and Han [13].

The physical properties of air in the numerical procedure were treated as constants and evaluated at the inlet temperature T_0=293 K, as ρ =1.205 kg/m^3, μ =1.81x10^{-5} kg/m-s, Cp=1005 J/kg-K, k_f =0.0259 W/m-K, and β = 0.00341 K^{-1}. The thermal conductivity of the back step was set equal to k_s=386 W/m-K.

The flow rate at the duct entrance was fixed such that the Reynolds number (Re) was 200 for all the numerical simulations. The Reynolds number was computed based on the inlet bulk velocity U_o and the channel height. The effects of the buoyancy forces on the velocity field and the temperature distribution was studied by varying the Richardson number from Ri=0 to 3 and then selecting the appropriate value for the bottom wall temperature (T_w).

A finite volume technique was implemented for discretizing the momentum and energy equations inside the computational domain. The SIMPLE algorithm was used to link the pressure and velocity fields. Solution to the one-dimensional convection-diffusion equation at the control volume interfaces was represented by the power law [14]. Velocity nodes were located at staggered locations for each coordinate direction while pressure and temperature nodes as well as other scalar properties were placed at main grid nodes.

A combination of line-by-line solver and Thomas algorithm was implemented for each plane in x, y, and z coordinates direction for the computation of the velocity components, pressure, and temperature inside the computational domain. To ensure convergence when solving the mixed convective flow over a three dimensional horizontal backward facing step a severe under-relaxation for the velocity components ($\alpha_u=\alpha_v=\alpha_w$=0.4), pressure ($\alpha_p$=0.4) and temperature ($\alpha_T$=0.4) was imposed. Convergence was declared when the normalized residuals for the velocity components and pressure were less than 10^{-8}. For the temperature the stop

criterion required that the maximum relative change in the temperature domain should be less than 10^{-6}.

A variable grid size was considered for solving the problem. The grid used in this work was very fine near the walls of the channel and close to the step. A non-uniform grid was deployed by using a geometric expansion factor. The grid independence study was conducted by using several grid densities for the most severe parametric values (Ri=3 and Re=200) considered in this study. The average Nusselt number distribution (Nu) and the maximum velocity (u_{max}) at the channel exit were monitored to declare grid independence.

A grid size of 100x40x40 was chosen as the base case. Then several tests were conducted by varying the expansion factor in the z direction as is shown on Table 1. A negligible percentage deviation was found for the expansion factor e_z=1.2. An increase in the grid size in x and y direction presented differences no larger than 1.0%.

The lack of previous experimental or numerical data in the literature for the problem in question precludes the direct numerical validation of the numerical code developed for solving the mixed convective flow over a three dimensional horizontal backward facing step. Hence, two closely related problems to the mixed convective flow over the three dimensional backward facing step were considered to validate the numerical code developed for this research. For each verification test the hydrodynamic and thermal flow features were compared with the previously published literature.

Table 1 Grid independence study

Grid Size (x*y*z):(100*40*40)

Expansion factor (x-y):(1.025-1.35)

Expansion factor for Z	Nusselt average at exit	% diff	u-max at exit	% diff
Uniform grid	4.7743		0.1248	
1.04	4.5016	6.05	0.1326	5.91
1.08	4.1798	7.69	0.1324	0.11
1.10	4.0263	3.81	0.1326	0.08
1.12	3.8812	3.73	0.1326	0.0
1.14	3.7462	3.60	0.1324	0.15
1.16	3.6223	3.42	0.1323	0.07
1.18	3.5098	3.20	0.1322	0.07
1.20	3.4085	2.97	0.1322	0.0

Test case #1

The first test case was that for simulating pure forced convective flow over a three-dimensional backward facing step subjected to constant heat flux heating along the bottom wall [6]. The numerical predictions of reattachment lengths and Nusselt number distributions using the developed code was compared with the experimental data for Re=343 and numerical predictions for Re=400 presented by Nie and Armaly [6]. The comparisons are shown in Figs. 2 and 3.

Due to the symmetry in the geometry the literature for pure forced convection presents values for half of the channel in the spanwise direction. However, this assumption was not considered in this research and computations were made by considering the entire spanwise width of the channel. In order to be consistent with the format in the reference cited, the results are presented for only half of the channel width in Figs. 2 and 3. The numerical predictions using the code developed for this research agree very closely with both the experimental and numerical results in the published literature as it is shown in Figs. 2 and 3.

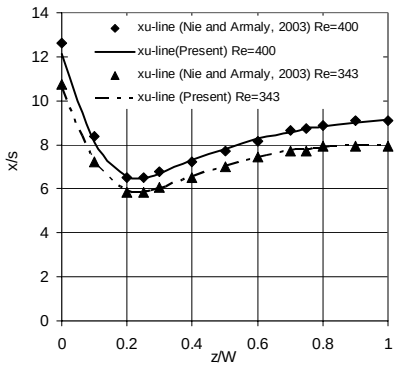

Fig. 2 x_u-line for the stepped wall z/W=0 : wall z/W=1 : central plane

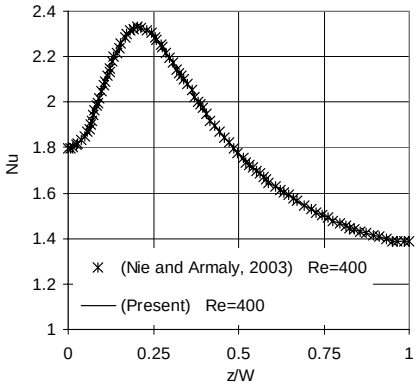

Fig. 3 Local Nusselt number distribution for the stepped wall at x/s=6.6 z/W=0 : wall z/W=1 : central plane

Test case # 2

The second test case was that of simulating mixed convective flow in straight horizontal channel with no blockage, heated from below by subjecting the wall to a constant temperature [15]. The channel's width to height ratio was equal to 2. The numerical predictions using the code developed for this research closely agreed with the numerical predictions in the literature as shown in Fig 4.

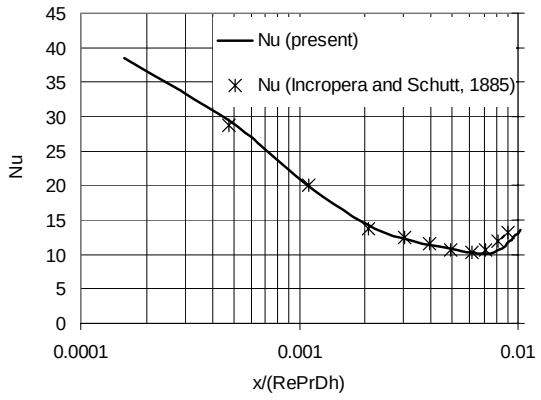

Fig. 4 Average Nusselt number for a mixed convective flow through a straight rectangular channel $Gr^*=11.40x10^6$ Re=500 Pr=0.71

RESULTS AND DISCUSSION

From experience it is known that the flow through the backward facing step channel is extremely sensitive to the abrupt geometrical change at the step. Downstream of the step and just behind the primary recirculation zone, the velocity profile is reattached and redeveloped approaching that of a fully developed flow as fluid flows towards the channel exit. However, the behavior described earlier for a pure force convective flow is completely distorted in presence of buoyancy forces. The last scenario considered is a mixed convective problem and is the central theme for this work.

The mixed convective flow is a process in which both the forced and the buoyant effects are of significant importance and primarily occurs in laminar and transitional flow regime. Therefore, for all numerical simulations considered in this study the Reynolds number (Re) was fixed to be Re=200.

The variation in buoyancy forces was accomplished by altering the imposed temperature along the bottom wall which in turn alters the Richardson number (Ri). Mixed convective effects on the flow were studied by simulating flows for three different Richardson numbers (Ri= 1, 2, and 3). When Ri=1 the forced and free convective forces are comparable and, if Ri increases, the free convective effects are dominant over forced convective effects in the flow. The extreme case in this study is for Ri=3, where the free convective effects are strongly prevailing over to the forced convective effects.

The mixed convective effects were studied by monitoring the so called x_u-line, the average Nusselt number, and some velocity profiles at specific planes by comparing with the results for mixed convective flow and those for pure forced convective flow.

In a two-dimensional flow over a backward facing step, the point where the shear stress is equal to zero is used to locate the reattachment length and to allocate the primary recirculation zone downstream of the step. However, for a three-dimensional flow the same definition represents a point in a horizontal plane and cannot be used to demarcate the recirculation zone. The common assumption for delimiting the recirculation zone in a three-dimensional case is the distribution in the spanwise direction for points in the axial direction where the streamwise component of the shear stress at the wall is equal to zero. Therefore the limiting primary recirculation zone is bounded by a line in the spanwise direction named the x_u-line.

Figure 5 shows the x_u-line for different mixed convective and pure forced convective flows. The x_u-lines present a symmetric behavior with respect to the middle plane in the spanwise direction. A minimum value is located approximately at z/W=0.2 and z/W=0.8. This effect is associated with the influence of the viscous effects and the no slip condition imposed at the lateral walls. The larger reattachment point is along the lateral walls.

For Ri=1 a very similar behavior as the pure forced convective flow is found. However, the location of x_u-line for mixed convective flow Ri=1 is pushed further downstream. The mixed convection in ducts presents two different structures or convective rolls, and depending on the effects of the mixed convection the rolls can be transverse or longitudinal in nature [16]. The onset of transverse rolls occurs at low Grashof numbers (Gr). Therefore for Ri=1, the presence of transverse rolls is the reason why the x_u-line is displaced downstream of the channel inlet (x/s=0).

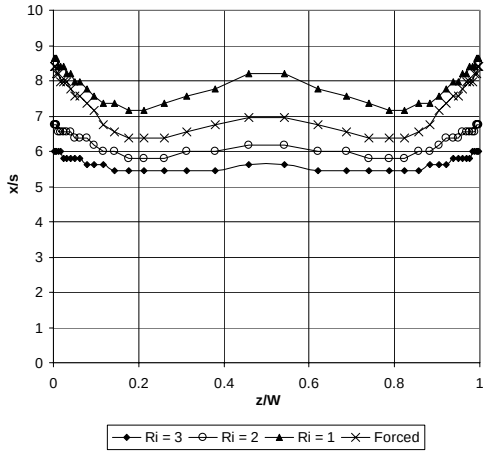

Fig. 5 x_u-line distribution for the 3-D backward facing step

On the other hand, for Ri=2 and 3 the location of x_u-line is upstream of the x_u-line location for Ri=0. It is evident from the Fig. 5, that when Ri increases the recirculation zone is shortened due to the presence of strong buoyant forces and higher v-velocity components in the vicinity of the heated wall.

The stream-wise-direction component for the average shear stress at the bottom wall is presented in the Fig. 6.

The negative values in Fig. 6 are associated with the primary recirculation zone, and the point where τ_{wx} changes to a positive value could be interpreted as "*the average reattachment point*". This point is shifted upstream if Ri is larger (Ri=3) and the farthest point downstream happens for Ri=1 as a consequence of the earlier discussion (following the Fig. 5).

The span-wise averaged Nusselt number distribution for the mixed convective flow in the channel with a backward step is presented in Fig. 7. The average Nusselt number distribution at the entrance of the backward facing step channel has a high value and then monotonically decreases. At the end of the step a dramatic change in the Nusselt number distribution was found due to the flow separation and the abrupt change in the channel geometry. Figure 7 shows a similar tendency for the Nusselt number distributions for the three mixed convective cases in consideration and the higher values are associated to higher Ri numbers.

The location of maximum Nu in the stream-wise direction shifts upstream with increase in Ri. For Ri=1, the location of maximum Nusselt number is found further downstream of the step (step ends at x=0.02) while for Ri=3 and 2 the location of maximum was found in the proximity of the step. After reaching a maximum value the Nusselt number decreases toward its fully developed value at the channel exit.

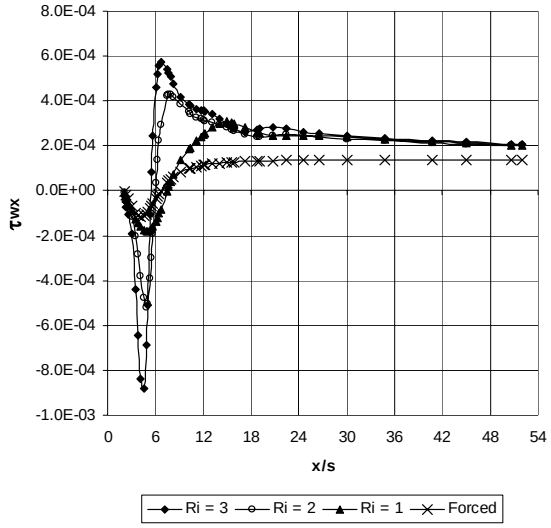

Fig. 6 Average stream-wise direction component for the shear stress

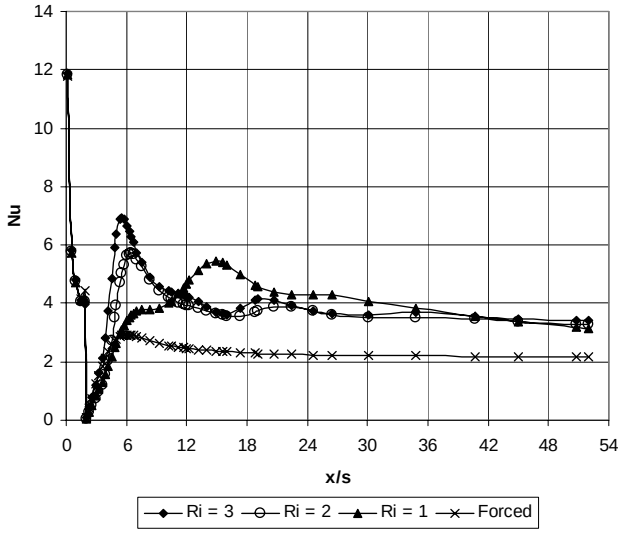

Fig. 7 Spanwise averaged Nusselt number distribution for the mixed convective flows over a 3-D backward facing step

It is also observed in this figure that after reaching the minimum value just behind the step, the Nusselt number distribution sharply increases to reach its maximum value inside the primary recirculation zone for Ri=3 and Ri=2. However for Ri=1 this value is delayed further this zone due to presence of transverse rolls as described earlier (Fig. 5).

According to Fig. 7 the average Nusselt number distribution for pure forced convective flow has a similar behavior as the mixed convective flow, but the average distribution values are considerably smaller for the pure forced convection than for mixed convection. The minimum value in the distribution for forced convection happens just behind the step and its maximum is reached inside the primary recirculation zone. After that the value decreases monotonically towards its fully developed value at the channel exit.

Velocity distributions for each of the velocity-components are presented in Fig. 8 in order to study the influence of the buoyancy forces on the fluid flow field. Figure 8 shows the u velocity component for the central plane in the span-wise direction (z/W=0.5) at several x-planes for pure forced convective flow and dominant mixed convective flow. As previously mentioned at the inlet (x=0) the flow is considered as hydrodynamically fully developed for all the numerical simulations.

In the vicinity of the step at x=0.02, the u velocity component has a slight deviation from the hydrodynamically fully developed flow values and the velocities at this point are slightly less than that for x=0 in the region above the step. Also, u values were negative near the bottom of the channel and this effect is most pronounced for the case of Ri=3.

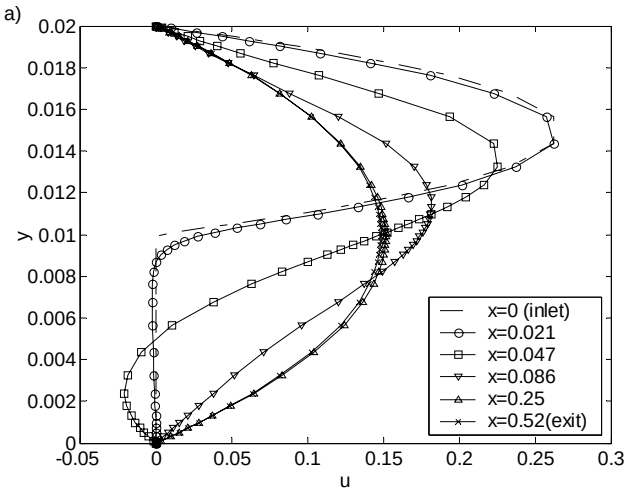

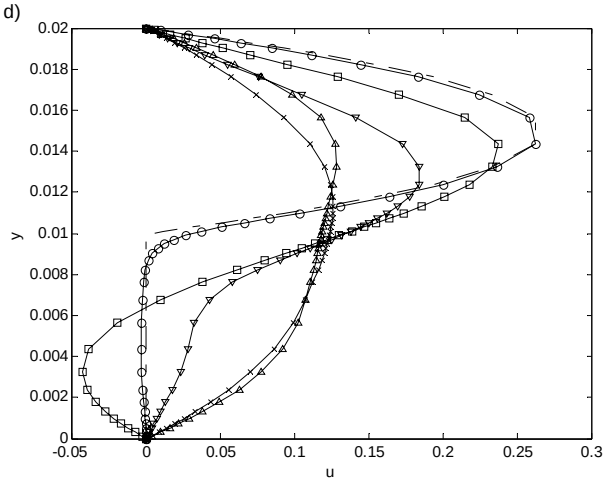

Fig. 8 u- velocity profiles at plane z=0.02 at different x positions
a) Forced convection, b) Ri=3, c) Ri=2, d) Ri=1

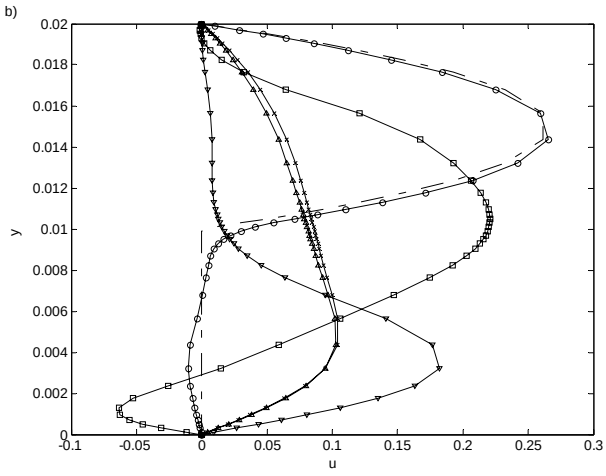

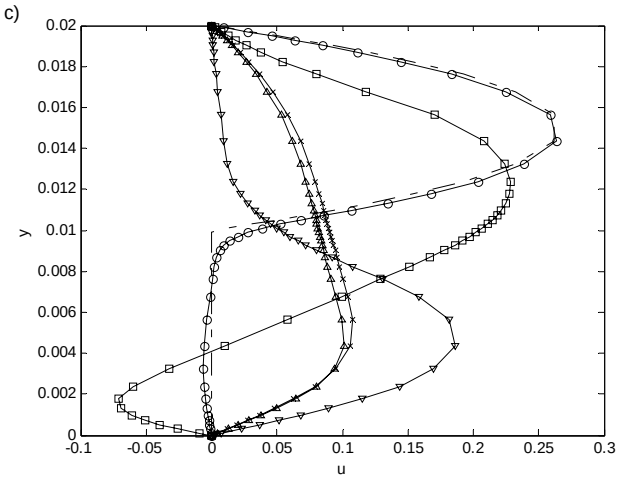

At a constant value x=0.047 the recirculation of the flow becomes evident along the bottom of the channel. Also, the negative value of u next to the bottom wall of the channel increases with increase in Ri. On the other hand the maximum value of the u component in the positive direction occurs for the pure forced convective flow. As Ri increases, the vertical size of the recirculation zone is reduced. This effect is related to the buoyant forces in the flow.

Figure 8(b) reveals the presence of a small recirculation zone attached to the roof of the channel at x=0.047 and the effect is extending until x=0.086. This effect was found only for the Ri=3 and is due to the strength of the mixed convective flow in this case. The u velocity profile at x=0.25 (half of the channel in the streamwise direction) reveals that for pure forced convective flow the u velocity component begins to show a fully developed behavior. For Ri=1 the u-velocity components tends to approach fully developed velocity profile. For Ri=3 and Ri-2 the velocity profile behavior is very different from a fully developed flow. The maximum in the velocity profile is shifted towards the bottom of the channel.

It is evident from Fig. 8 that the length of the channel is long enough to accommodate fully developed flow for pure forced convection (Ri=0). None of the mixed convective flow cases considered in this study was able to reach the hydro-dynamically fully developed conditions at the channel exit. The case of Ri=1 was the one of the mixed convective cases that appeared to be approaching fully developed flow conditions at the channel exit. The u-velocity components at the channel exit for mixed convective cases were found to be non-symmetric respect to the y axis.

Figure 9 presents the v-velocity distribution. In these figures, the plane y=0.01 is the central plane while y=0.004 is a plane near the bottom wall and y=0.0198 is a plane near the top wall. The magnitude of the velocity v-component is extremely small near the top and bottom walls. It should be noted that higher values for the v-component are for Ri =3 where the buoyancy effects dominate.

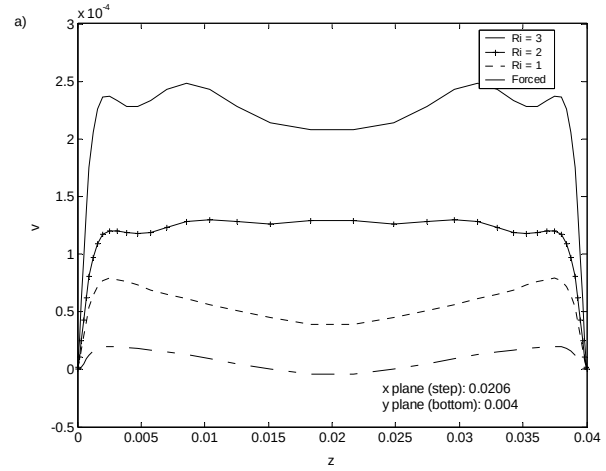

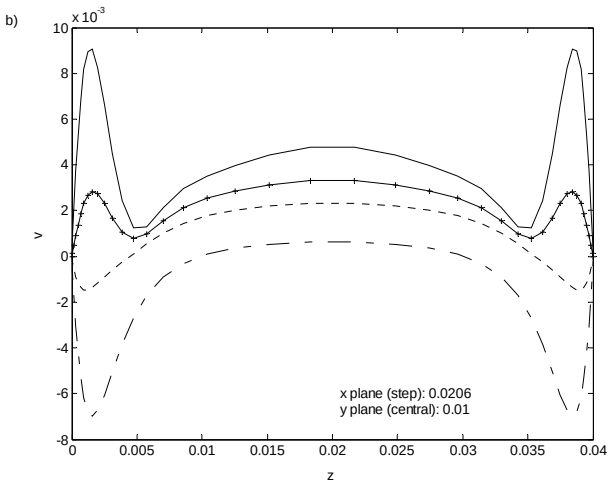

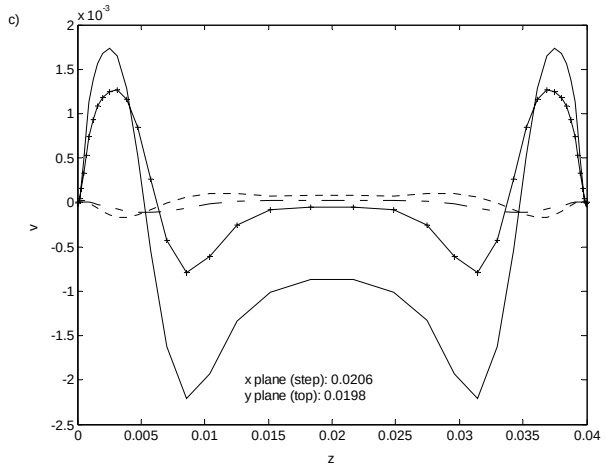

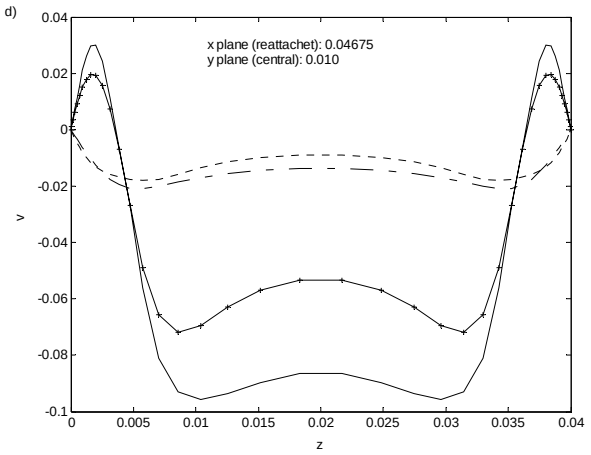

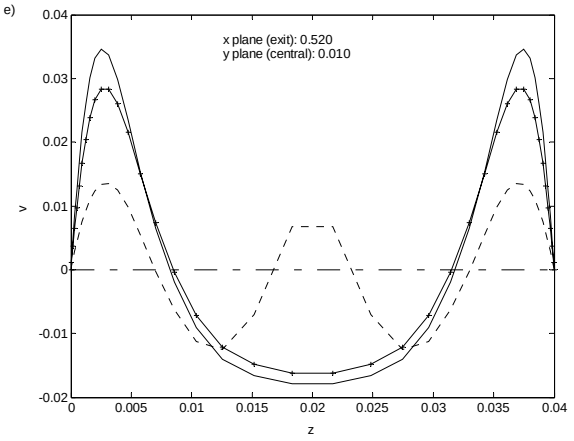

Fig. 9 v-velocity at different x and z constant planes

Figure 9(a) shows that for Ri=3 the v-velocity component values are three times larger than the values for pure forced convective flow. This effect is associated with the strength of the mixed convective flow as it was mentioned before; the effect of mixed convection is to reduce the size of the recirculation zone in both streamwise and vertical directions.

Figure 9(b) shows that at the edge of the back step, the line for pure forced convection does not have positive values for the v-velocity component, but the lines for Ri=3 and Ri=2 have the opposite behavior. In others words, at the edge of the step for pure forced convection the flow is descending while for mixed convection the flow is ascending due to the buoyant forces.

Figure 9(c) shows that at the top of the channel the v-velocity has negative values along the spanwise direction except for a small region near the side walls where the values are positive.

Figure 9(d) shows the v-velocity at x constant plane inside the primary recirculation zone and at the central constant y plane in the vertical direction. For Ri=3 and Ri=2 the afore mentioned effect of ascending flow near the side walls is observed. However, at the channel central region in the z-direction the v-velocity distribution shows high negative values indicating that the flow is directed towards the bottom wall. This is the reason why the recirculation zone is not only reduced in the streamwise direction but also in its transversal direction (y-direction).

Figure 9(e) confirms that at the channel exit the flow is fully developed for pure forced convective flow (v=0) and that for mixed convective flow, the v-component of the velocity has considerable non-zero values. This figure also shows that for strong mixed convective flow (Ri=3 and Ri=2) positive values for the v-velocity component are present near the side walls and negative values are present in the middle of the channel. This is the reason why the maximum of u-velocity component in the central plane is shifted towards the bottom wall as seen in Figs. 8(b) and 8(c).

Figure 10 presents the spanwise w-velocity distribution at different planes. It is evident in Fig. 10 that for pure forced convective flow the change in the w-velocity component is minimal and the variation in w-component in the spanwise direction is greater near the walls than in the middle of the channel. This behavior is associated with the formation of convective rolls in the flow. Even though the variation in the w-velocity component is minimal, this component cannot be neglected in the numerical discretization in order to save computational effort.

As expected, the higher values for the w-component velocities are associated with larger Ri values. In the vicinity of the back step (Figs. 10(a) and 10(b)) the w-component of the velocity has extremely small values. Higher values for the w-velocity component are present downstream of the backstep (Figs. 10(c) and 10(d)).

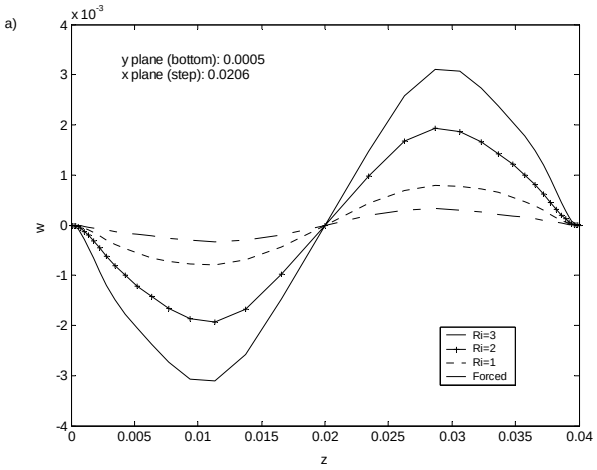

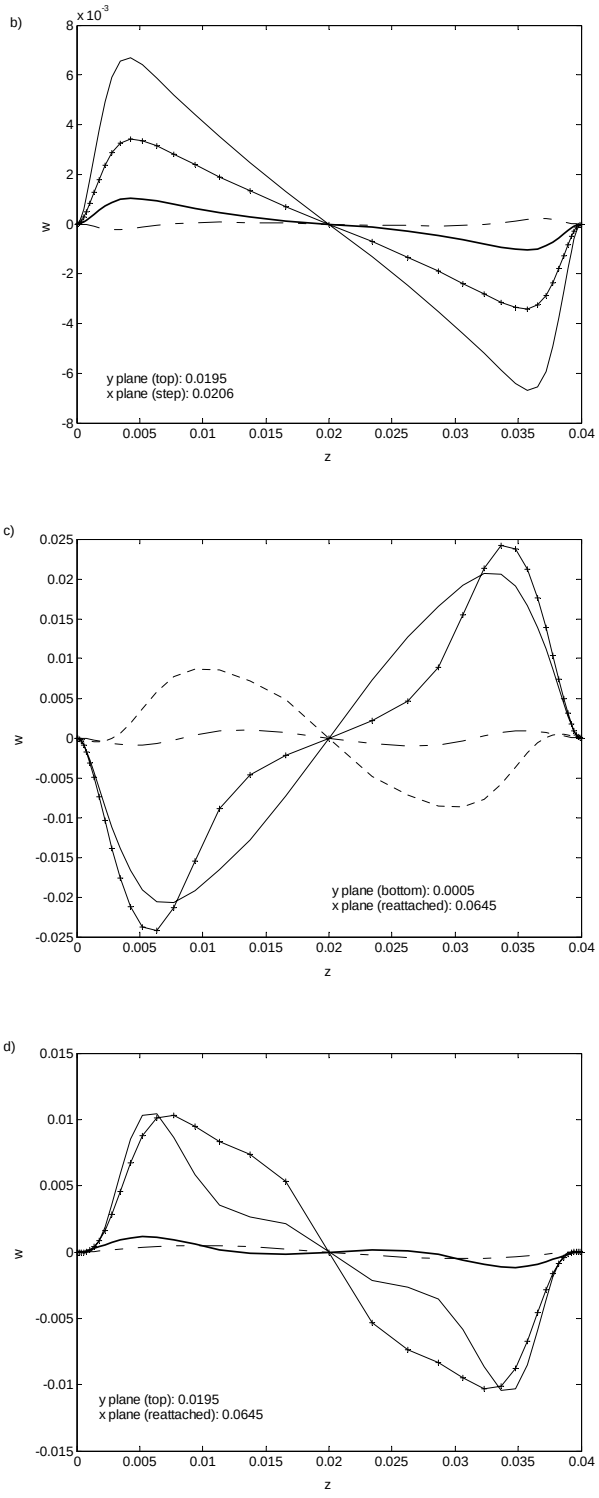

Fig. 10 w-velocity component at different planes

Analyzing the Fig. 10 and considering the coordinate system proposed in Fig.1, it is evident that at the top of the channel the w-velocity component acts towards the central plane in the spanwise direction (z=0.02), while at the bottom wall the flow is directed towards the side walls.

Figure 11 presents the temperature contours and the vector velocity component at x=const plane for the convective flows considered in this study. A pair of longitudinal convective rolls is perfectly defined by Ri=3 and Ri=2 in Figs. 11(a) and 11(b). It is evident that the flow is ascending by the side walls and is moving towards the bottom wall near the middle plane in the spanwise direction (z=0.02). As a result, in Figs. 8(b) and 8(c) the maximum for the u-velocity component at the channel exit is shifted towards the bottom wall. For Ri=1 the longitudinal vortices are not completely defined even though the velocity structures tends to align with longitudinal vortices. For the pure forced convective case in Fig. 11(d) the flow structures do not show formation of the convective rolls, but they resemble a fully developed flow.

The temperature contours show the presence of high temperatures along the channel roof. According to the linear relationship between density and temperature this is an expected behavior. Flow with lower density and high temperature must be along the top wall of the channel. For the pure forced convective case the temperature contours reveal that the region of high temperature is near to the heating zone.

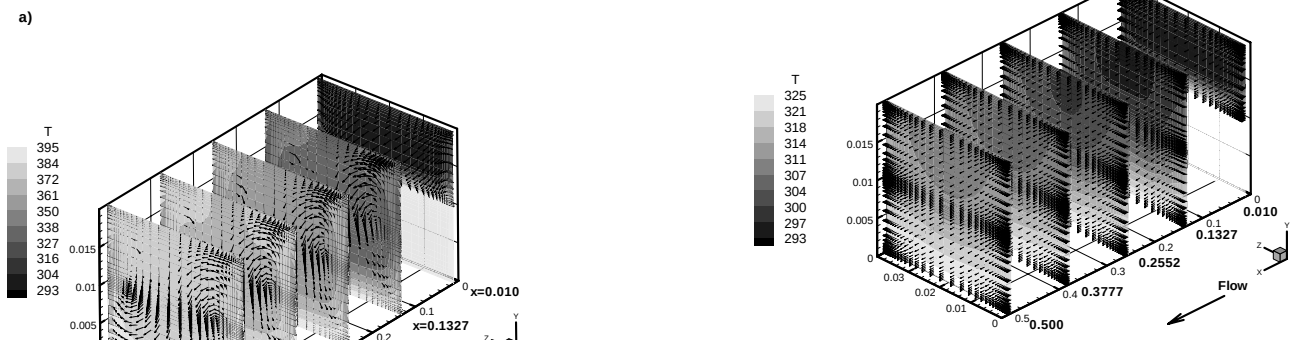

Fig. 11 Temperature contours and velocity vectors at constant x planes
a) Ri=3, b) Ri=2, c) Ri=1, d) Forced convection

The influence of the conducting block on the mixed convective flow was studied for blocks with different thermal conductivity. Figure 12(a) shows the temperature distribution inside the block at the central plane in the spanwise direction for k_s=386 (Cupper). Figure 12(b) shows similar information for k_s=64 (Carbon steel AISI 1010).

The thermal conductivity in the block does not impact the temperature distribution for the mixed convective flow and the only effect is on the temperature distribution inside the back step. Even though the temperature gradients inside the block can be neglected it was observed that a higher temperature gradient exists for the smallest thermal conductivity. It is important to mention here that the geometrical dimensions for the back step in the streamwise direction (x direction) is two times the step height while the total length of the channel is 52 times the step height.

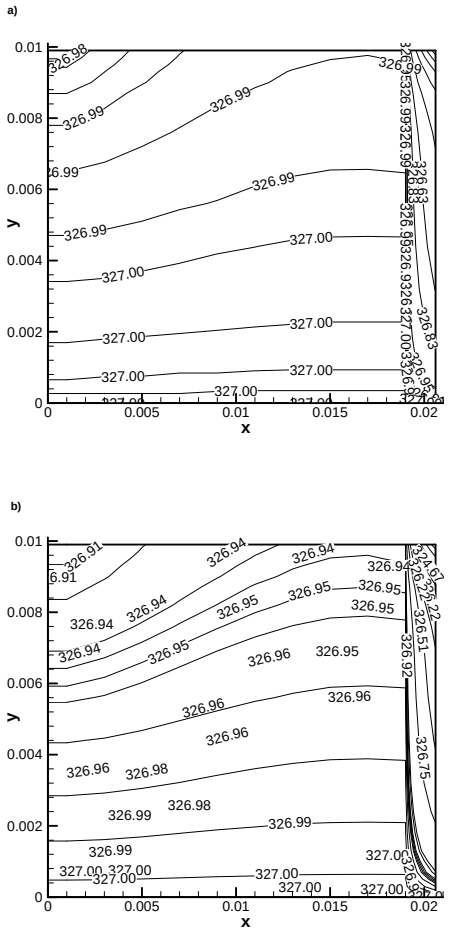

Fig. 12 Temperature distribution inside the back-step for the central plane z=0.02 a) k_s=386 (Cupper) b) k_s=64 (Carbon steel AISI 1010)

CONCLUSIONS

The mixed convective flow over a three dimensional horizontal backward facing step heated at constant temperature from below was numerically simulated via a finite volume technique.

Four different degrees of buoyancy effects ranging from pure forced convective flow to mixed convective flow were considered (Ri=0, 1, 2, and 3). The numerical results show that the features of the mixed convective flow are significantly different from that of forced convective flow, which affects the velocity field and temperature distribution.

The location of the maximum value of spanwise average Nusselt number moves upstream with increase in Ri. Increase in the mixed convective parameter (Ri) decreases the size of the primary recirculation bubble in both streamwise and vertical directions.

REFERENCES

[1] Iwai, H., Nakabe, K., Suzuki, K., and Matsubara, K., 2000, "Flow and heat transfer characteristics of backward-facing step laminar flow in a rectangular duct," International J. Heat and Mass Transfer, **43**, pp. 457-471.

[2] Iwai, H., Nakabe, K., Suzuki, K., and Matsubara, K., 2000, "The effects of duct inclination angle on laminar mixed convective flows over a backward-facing step," International J. Heat and Mass Transfer, **43**, pp. 473-485.

[3] Nie, J. H., and Armaly, B. F., 2002, "Three-Dimensional Convective Flow Adjacent to Backward-Facing Step –Effects of step height," International J. Heat and Mass Transfer, **45**, pp. 2431-2438.

[4] Blackwell, B.F., and Pepper, D.W., 1992, Benchmark problems for heat transfer codes, ASME-HTD-**222**, ASME, NY.

[5] Armaly B. F., Li, A., Nie, J. H., 2003, "Measurements in three-dimensional laminar separated flow," International J. Heat and Mass Transfer, **46**, pp. 3573-3582.

[6] Nie, J. H., and Armaly, B. F., 2003, "Reattachment of three-dimensional flow adjacent to backward-facing step", ASME J. Heat Transfer, **125**, pp. 422-428.

[7] Nie, J. H., and Armaly, B. F., 2002a, "Buoyancy effects on three-dimensional convective flow adjacent to backward-facing step," AIAA J. Thermophysics and Heat Transfer, **17**, pp. 122-126.

[8] Carrington, D. B., and Pepper, D. W., 2002, "Convective heat transfer downstream of a 3-D backward-facing step," Numerical Heat Transfer, Part A, **41**, pp. 555-578.

[9] Li, A., and Armaly, B. F., 2000, "Mixed convection adjacent to a 3-D backward facing step," HTD- Proceedings of the ASME Heat Transfer Division, **2**, pp. 51-58.

[10] White, F. M., 1991, *Viscous Fluid Flow*, 2nd ed., McGraw-Hill, USA

[11] Kakac, S., and Yener, Y., 1995, *Convective Heat Transfer*, 2nd ed., CRC Press, Inc, USA

[12] Shah, R.K., and London, A.L., 1978, *Laminar flow forced convection in ducts*, Academic Press, New York, USA

[13] Xi, C and Han, P., 2000, "A Note on the Solution of Conjugate Heat Transfer Problems Using SIMPLE-like

algorithms", International J. of Heat and Fluid Flow, **21**, pp 463-467.

[14] Patankar, S. V., 1980, *Numerical Heat transfer and Fluid Flow*, Taylor and Francis, USA

[15] Incropera, F. P., and Schutt, J. A., 1985, "Numerical Simulation of Laminar Mixed Convection in the Entrance region of Horizontal Rectangular Ducts", Numerical Heat Transfer, **8**, pp. 707-729.

[16] Luijkx, J.M., Platten, J.K., and Legros, J.CL., 1981, "On the existence of thermoconvective rolls, transverse to a superimposed mean Poiseuille flow," International J. Heat and Mass Transfer, **24**, pp 1287-1291.